458 KSME Journal, Vol. 10, No. 4, pp. 458~470, 1996

The Effect of Non-Orthogonal Grids on Spray and Air Flow Predictions

K. Park* and A. P. Watkins**

(Received August 30, 1995)

This paper describes the effect of non-orthogonal grids on both spray and air flow predictions, and the effect of higher order convection scheme on inclined grids. In order to assess the effect of non-orthogonality of grids a number of different grid cases are generated, and applied to the same conditions of injected sprays. The effects on the free/wall spray penetration and Sauter mean diameter(SMD) are discussed. The results show that the numerical error is increased with increasing non-orthogonality, and that Hybrid is better than QUICK for the calculation of sprays on inclined grids. For the calculation of the spray injection, which has always large gradient regions at the front end, adaptive grids following the direction of spray/gas flow might be required.

Key Words: Non-Orthogonality, Spray, Grid Generation, Angled Grid

1. Introduction

Nowadays pollution by vehicles has become the main source of city air pollution. A large part of that is caused by diesel vehicles. Diesel engines have a basic spray injection which is not homogeneous but has a thick core in each spray. To reduce pollution problem, various methods are used in the areas of injection systems, intake/exhaust systems, combustion chambers, etc. As one of the ways, shaped engines using wall impaction of sprays have recently been proposed and given good results.

The main purpose is in breaking up the core of the spray and directing the spray in a desired direction, so that the spray is easily able to mix with air and atomize into smaller drops. First Kroeger(1986) presented a shaped combustion chamber system using methanol. Soon after a similar chamber system was designed by Kato and Onishi(1987), with later developments (1990). Park et al(1993) and Ogura and Lin (1994) proposed other types of chamber systems with multi-hole injectors and corresponding impingement sites. The shapes of these chambers have very complicated boundaries. As a result the computational grids generated to calculate the in-cylinder flow are very distorted. Numerical losses on such grids have to be considered.

In this paper the loss or error by non-orthogonality of grids is discussed, and as a result the limit of the distortion rate of grids is proposed. The convection scheme used for calculation of sprays on inclined girds is discussed as well.

* Korea Institute of Machinery & Materials
** University of Manchester Institute of Science and Technology

2. Mathematical Model

For the gas phase the transport equations for mass, momentum, specific energy, fuel vapour mass fraction, turbulence kinetic energy k and its dissipation rate ε can be written in the following general form with the effects of fuel sprays taken into account;

$$\frac{\partial}{\partial t}(\theta b\Phi)+\nabla\cdot(\theta\rho\bar{V}\Phi)=\nabla\cdot(\theta\Gamma_{\Phi}\nabla\Phi)+\theta S_{\Phi}+S_{\Phi}^{d} \quad (1)$$

where the super script d stands for the liquid phase, ρ is the gas density, $\bar{V}$ is the gas phase velocity vector, Γ_{Φ} and S_{Φ} are the diffusion

coefficient and the source term respectively for each Φ which is a conserved property such as u^i, e, f, k, ε and 1 for the continuity equation. The void fraction θ is defined as the volume fraction of gas in each cell, that is

$$\theta = 1 - \frac{\Delta V_{liquid}}{\Delta V_{cell}} \tag{2}$$

where ΔV_{cell} is the cell volume and ΔV_{liquid} is the volume of liquid in the cell.

These equations are transformed into general non-orthogonal curvilinear coordinates, then discretized using two convection schemes, Hybrid and QUICK. The transient term is expanded in the first order fully implicit form.

For the liquid phase, following Crowe et al (1977), Dukowicz(1980) and Gosman et al (1980) the liquid phase is modelled by the Discrete Droplet Model(DDM), in which a spray can penetrate and interact with the gas phase. Each calculated droplet represents a parcel containing many thousands of drops having the same size, temperature, velocity components, etc. If enough different droplet parcels are selected during injection, the distributions of drop sizes, velocity components and so on in the spray can be adequately covered. The models are explained carefully by Watkins(1989) and Khaleghi(1990).

The drop-wall interaction model has been introduced, which was based on experiments of individual drops. The model has been applied for boundary fitted general non-orthogonal grids. And it has been assessed through comparison with experiments over a wide range of conditions including different gas pressure, temperature and wall distance in the paper by Watkins and Park (1996).

3. Test and Discussion of Grid Non-Orthogonality

Usually the non-orthogonal code is developed to apply for cases with complicated boundary shapes, thus the grid can be very distorted. In this section the loss or error produced by non-orthogonality of grids is discussed, and as a result the limit of the distortion rate of grids is proposed.

To test the code, a number of different non-orthogonal grids are generated, and the numerical results using these non-orthogonal grids are compared with those from an orthogonal grid. The results used for comparison purposes are the penetration in free sprays, the SMD and wall spray radius and height.

3.1 Grid generation

Ten different grids are generated. First the orthogonal 20×20 grid is generated, Fig. 1(a), which is the base for all the others. The grid spaces between nodes in each direction are the same thoughtout, in order to eliminate the effects of variable grid spacings. Then three cases of horizontally distorted grid are defined(Fig. 1(b)). They are generated by 10%, 20%, 30% distortion of the distance between neighbouring grids as;

$$x^h_{i,j} = x^o_{i,j} \tag{3}$$
$$r^h_{i,j} = r^o_{i,j} - xx\,(r^o_{i,j} - r^o_{i,j-1}) \tag{4}$$
$$x^h_{i+1,j} = x^o_{i+1,j} \tag{5}$$
$$r^h_{i+1,j} = r^o_{i+1,j} \tag{6}$$

Where i is an even number, the superscripts h, o stand for the horizontally distorted grid and the orthogonal grid respectively, and xx is the distortion rate ($xx=0.1$, 0.2 or 0.3).

The three vertically distorted grid cases(Fig. 1(c)) are given in a similar way;

$$x^v_{i,j} = x^o_{i,j} - xx\,(x^o_{i,j} - x^o_{i-1,j}) \tag{7}$$
$$r^v_{i,j} = r^o_{i,j} \tag{8}$$
$$x^v_{i,j+1} = x^o_{i,j+1} \tag{9}$$
$$r^v_{i,j+1} = r^o_{i,j+1} \tag{10}$$

Where j is an even number, the superscript v stands for the vertically distorted grid, and xx is the distortion rate($xx=0.1$, 0.2 or 0.3).

And the other three cases are distorted both horizontally and vertically;

$$x^{hv}_{i,j} = x^o_{i,j} - xx\,(x^o_{i,j} - x^o_{i-1,j}) \tag{11}$$
$$r^{hv}_{i,j} = r^o_{i,j} - xx\,(r^o_{i,j} - r^o_{i,j-1}) \tag{12}$$
$$x^{hv}_{i+1,j} = x^o_{i+1,j} \tag{13}$$
$$r^{hv}_{i,j+1} = r^o_{i,j+1} \tag{14}$$

Where i, j are even numbers, the superscript hv stands for the horizontally and vertically distorted

grid, and xx is the distortion rate ($xx=0.1, 0.2$ or 0.3).

3.2 Test cases

Three cases are selected, which are listed in Table 1. All three cases have the same wall distance (24mm) to remove the effects of different overall grid spacings. Two cases (G1, G1) differ in gas pressure only and the other case (G3) is at high temperature and pressure.

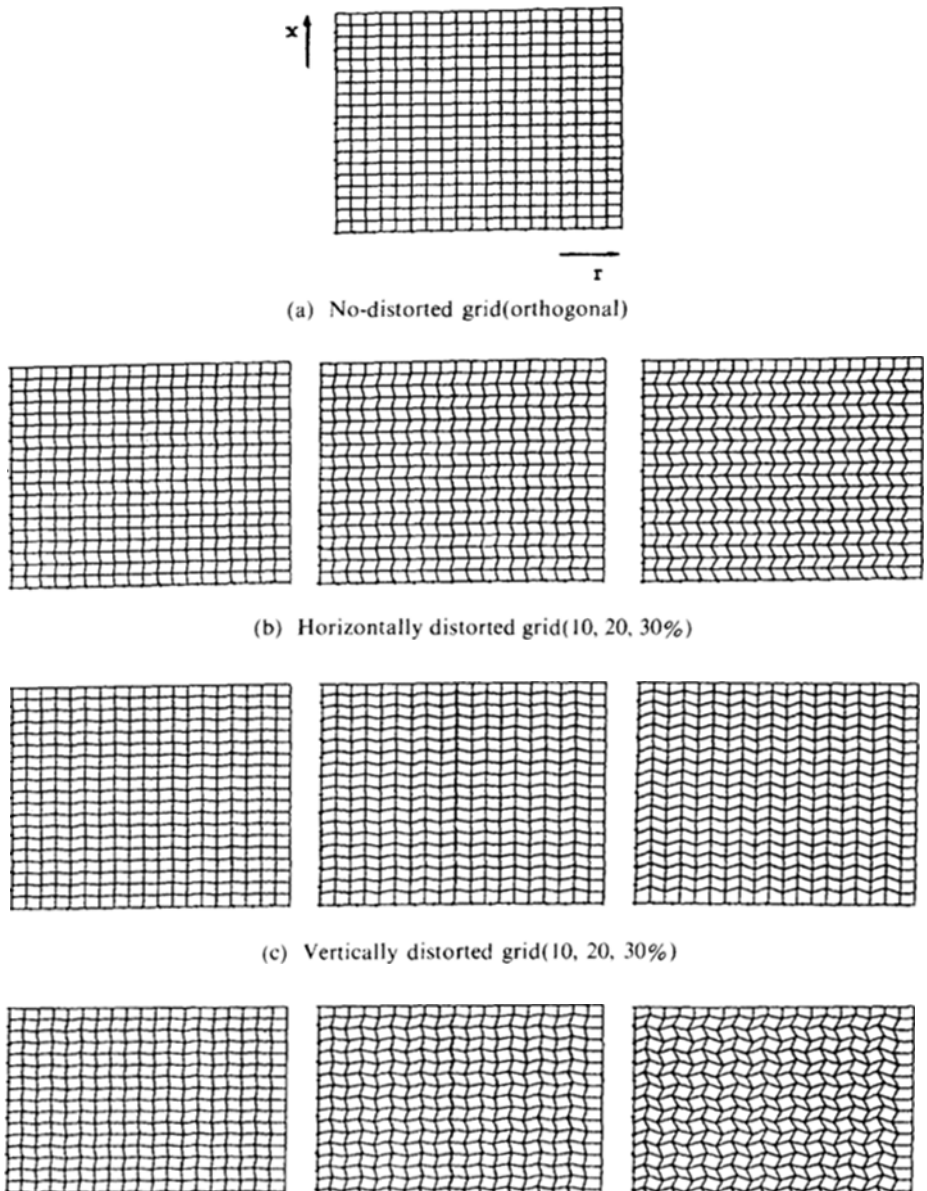

(a) No-distorted grid(orthogonal)

(b) Horizontally distorted grid(10, 20, 30%)

(c) Vertically distorted grid(10, 20, 30%)

(d) Horizonatally and vertically distorted grid(10, 20, 30%)

Fig. 1 Grids to test non-orthogonal code

Table 1 Test cases

Test cases	G1	G2	G3
Wall distance(mm)	24	24	24
Trap. pressure(MPa)	1.0	1.5	2.5
Trap. temperature(K)	Room	Room	700
Injection pressure(MPa)	14.0	14.0	16.4
Nozzle diameter(mm)	0.3	0.3	0.2
Injection duration(ms)	1.2	1.2	1.8

Table 2 Velocities at 0.3ms from injection(m/s)

Velocities	G1-1	G1-2	G1-3	G1-4
$V_{radius}(4,2)$	0.1	-4.2	0.1	-4.1
$V_{radius}(5,2)$	0.1	4.1	0.1	4.2
$V_{axial}(4,2)$	10.6	15.6	10.6	15.8
$V_{axial}(5,2)$	14.8	13.7	14.8	13.6

3.3 Discussion - cases G1, G2, G3 -

Ten different grids are employed in each case. As a matter of convenience they are described Gn -1 to Gn-10; three of them(Gn-2, Gn-3, and Gn -4) are horizontally distorted by 10%, 20%, 30% respectively, three(Gn-5, Gn-6, and Gn-7) are vertically distorted by 10%, 20%, 30% and the other three(Gn-8, Gn-9, and Gn-10) are horizontally and vertically distorted. These 9-cases are compared with the base grid Gn-1 without any distortion(orthogonal) and also compared to experimental results.

The wall spray distributions of G1-1 are compared to the photographs by Fujimoto et al. (1988) in Fig. 4(a),(b). In their experimental results the spray shape close to the impinging site is not shown clearly because of overlapping with the surrounding spray, however it is clear from their discussion that closer to the impinging site the wall spray gets thinner and a concave region is formed in the join of the free and wall sprays. Near the front of the wall spray droplets spread out and are formed into a vortex shape. Comparing with experiments the wall spray radius and height from the simulation are slightly underpredicted, however the spray shapes are in good agreement.

The calculated overall spray shapes on the ten different grids do not show any large differences, in particular the sprays before impact have very similar shapes. As can be seen in Fig. 2, some differences can be observed later at the front end of the wall spray. It can also be seen that the SMD varies by a small percentage value. The main differences are that the front end of the wall spray in the case of distorted grids tend to rise up and have reduced penetration.

Shown in Fig. 3 are the gas flow shapes of the four cases(G1-1, G1-4, G1-7, G1-10) which are no distortion, 30% horizontal, 30% vertical and

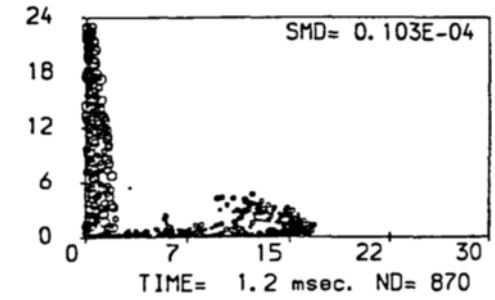

(a) Case G1-1

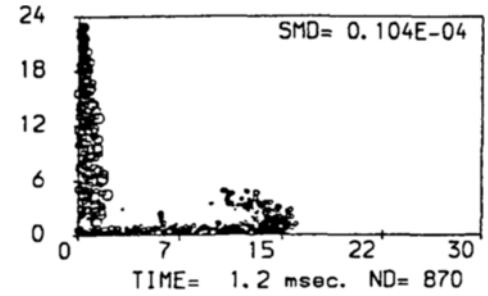

(b) Case G1-7

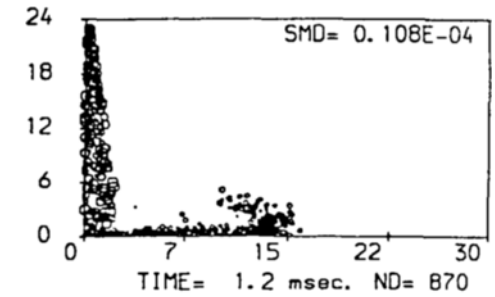

(c) Case G1-10

Fig. 2 Droplet distributions at 1.2ms from injection

30% horizontal and vertical distortion respectively. Shown in Table 2 are the velocities at the neighbouring cells of the centre line (4, 2) and (5, 2) which have large mass flow rates. Both show that the gas velocities in the field are dependent upon the shapes of grids.

For horizontally distorted grid G1-4, the gas velocities in the free spray are distributed such that they tend to follow the shape of the grid and it is clear the gas velocity field gets diffused more than in the orthogonal grid case G1-1.

Looking carefully at the neighbouring cells of the centre line, it is seen that the gas flows in and out repeatedly (Fig. 5(b) compared to 5(a)). The reason for this is explained in Fig. 5(c). High velocity flow in the jet region crosses the south cell face and induces a flow across the face with the sloped boundary. The coefficient value of south cell face, A_s, in the discretized algebraic equation are given as;

$$(A_s)_{ij} = \cdots\cdots + (P_{21})_{si}\rho u_{si} \quad (15)$$

$$(A_s)_{i+1j} = \cdots\cdots + (P_{21})_{si+1}\rho u_{si+1} \quad (16)$$

and

$$(P_{21})_{si} > 0 \quad (17)$$

$$(P_{21})_{si+1} < 0 \quad (18)$$

$$u_{si},\ u_{si+1} \gg 0 \quad (19)$$

Where the subscripts ij, si stand for ij-cell respectively and south surface of ij-cell, and P_{21} is the area vector component in u-direction on south face. The values u_{si}, u_{si+1} are very big compared with the other values. Thus the velocities in r-direction v_{ij}, v_{i+1j} are very effected by $(A_s)_{ij}$, $(A_s)_{i+1j}$ values and the gas flows in and out repeatedly.

The gas velocity fields look to be in disorder, but the flow moves regularly, i. e. the gas flows out on the south face of the ij-cell goes in on the south face of the i+1j-cell. Thus the whole shape of the gas field is similar to that of the case G1-1, but some loss may be expected in the axial direction during the process instead of some gain in the radial direction. This appears as more diffusion.

In the case of the vertically distorted grid, after the spray impacts on the wall the flow becomes complicated by the same reason as in the free stream for the grid G1-4. In u-momentum calculation the amount of flow in east cell face is dependent on the grid of the east surface, because in the east face high velocity fields are built up by the wall jet flow.

By the effect of the coefficient A_E on east face, the gas flow through the cells in the neighbourhood of the wall rise up and down repeatedly, during this process it loses a little energy along the wall, and diffuses above the wall more than that of the base case G1-1. Also this seems to be the reason that the front end of the wall spray rises up in this grid rather than in the orthogonal grid, and the wall spray penetration is significantly reduced.

For the horizontally and vertically distorted grid case G1-10, the gas velocities are distributed in apparent disorder more than that of the horizontally distorted or vertically distorted cases. By the combined effects of the horizontally distorted

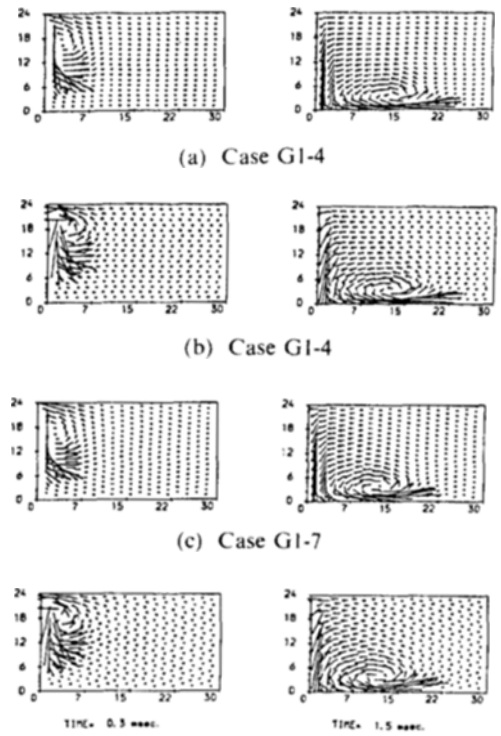

(a) Case G1-4

(b) Case G1-4

(c) Case G1-7

(d) Case G1-10

Fig. 3 Gas velocity fields at 0.3 and 1.5msec for case G1

grid and vertically distorted grid, the gas flows repeatedly in and out around the wall impaction spray as well as around the free jet stream.

The assessment of the effects of grid distortion on the free spray penetration is made by comparing the time to penetrate a distance of 24mm from the injector, i. e. the time in which the first droplet reaches the wall.

For the horizontally distorted grid cases (Gn-2, Gn-3, Gn-4), the time to penetrate to the wall increases in proportion to the distortion rate. For the vertically distorted grid cases (Gn-5, Gn-6, Gn-7) the time to reach the wall slightly decreases in proportion to its distortion rate. If the pattern of the vertically distorted grid is given

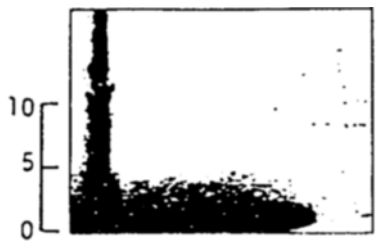

(a) Photograph by Fujimoto at 0.8ms from injection

(b) Simulation result at 0.8ms from injection

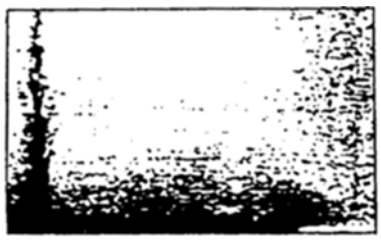

(c) Photograph by Fujimoto at 1.2ms from injection

(d) Simulation result at 1.2ms from injection

Fig. 4 Spray distributions of G1-.

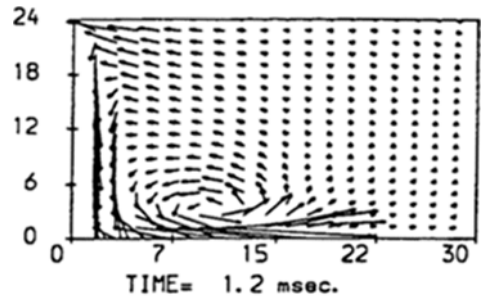

(a) Case G1-1

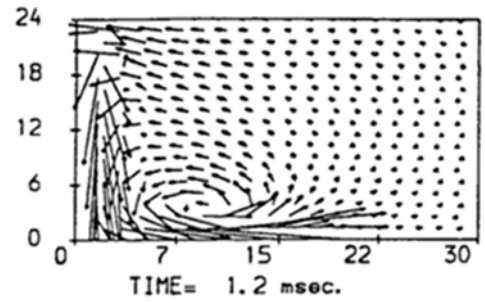

(b) Case G1-4

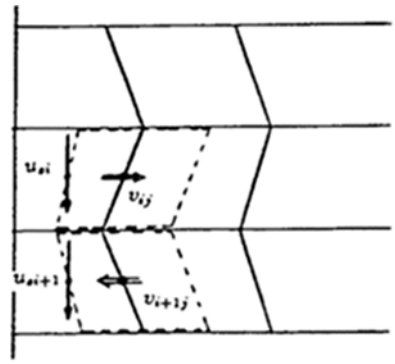

(c) Explanation

Fig. 5 Gas velocity fields at 1.2ms after injection

in the other way that has a reverse pattern of the present, then the velocity flow in the axial direction is reduced by the reverse effect. And for the horizontally and vertically distorted grid cases (Gn-8, Gn-9, Gn-10), the time to reach the wall slightly increases in proportion to its distortion rate, which tells that the effect of the horizontal distortion is more than that of the vertical.

For the free spray before impaction the values of SMD in all the cases of the horizontally distorted grid, the vertically distorted grid and the horizontally and vertically distorted grid are the same as the base value of Gn-1.

For the horizontally distorted grid cases (Gn-2, Gn-3, Gn-4), the values of SMD after wall impaction increase in proportion to its distortion rate. The increase of SMD with grid distortion after wall impaction seems to be caused by the droplet impaction velocity normal to the wall surface being reduced with distortion of the grid

For the vertically distorted grid cases (Gn-5, Gn-6, Gn-7), the value of SMD after the wall impaction slightly decreases contrary to the horizontally distorted case. And for the horizontally and vertically distorted grid cases (Gn-8, Gn-9, Gn-10), the size of SMD after the wall impaction increases like the horizontally distorted cases.

Wall spray radius (penetration along the wall) and height of the spray above the wall are checked at three times (0.9ms, 1.2ms, 1.5ms) after the injection for ten different grid cases.

For the horizontally distorted grid cases (Gn-2, Gn-3, Gn-4), the wall spray radii at all the three times (0.9ms, 1.2ms, 1.5ms) from the injection decrease in proportion to the distortion rate. And the wall spray heights distribute sporadically with the distortion rate; decrease for 10%, increase for 20% and decrease again for 30%.

For the vertically distorted grid cases (Gn-5, Gn-6, Gn-7), the wall spray radii decrease in proportion to the distortion rate, while the heights increase. For the horizontally and vertically distorted grid cases (Gn-8, Gn-9, Gn-10), the tendency of the variation of the wall spray radius and height is the same as that of the vertically distorted cases.

To assess the effect of the grid distortion on the total wall spray field, the percentage error (PE) including both the values of the wall spray radius and the height is introduced as;

$$PE_{radius+height} = \frac{(R_w + H_w)_{G1-i} - (R_w + H_w)_{G1-1}}{(R_w + H_w)_{G1-1}} \tag{20}$$

Where the Rw, Hw are the wall spray radius and height respectively and i is the grid cases ($i = 2, \ldots 10$) and G_{i-1} is the orthogonal grid.

The absolute value of the percentage error (PE) by *radius + height* can be regarded as the gross loss caused by the grid distortion and it is shown in Fig. 6.

For the horizontally distorted grid cases (G1-2, G1-3, G1-4), the gross loss increases with distortion rate; it remains less than 2% up to 20% distortion rate but suddenly increases up to 9% at 30% distortion rate. For the vertically distorted grid cases (G1-5, G1-6, G1-7), the gross loss is not proportional to the distortion rate, but increases slightly. For the horizontally and vertically distorted grid cases (G1-8, G1-9, G1-10), the gross loss increases in proportion to the distortion rate.

The main differences of the condition among the test cases G1, G2 and G3 are the gas temperature between G1 or G2 and G3 (G1, G2:room, G3: 700K) and the gas pressure between G1, G2 and G3 (G1:1.0MPa, G2:1.5MPa, G3:2.5MPa).

Case G2 exhibit a very similar tendency to the case G1 shown in previous discussion, but in case of G3 the results are disordered and different from the cases G1, G2. For all three cases, the horizontally distorted grid has given more loss than the vertically distorted one.

By looking at the percentage error adjusted to the 10% distorted grid compared with the orthogonal cases G_{N-1}, 0.07%-3.84% error for the horizontally, 0.2%−2.2% error for the vertically and 0.30% - 3.98% error for the horizontally and vertically distorted grid are shown in all the thirty cases (Three different test conditions with 10

different grids; G1-1, · · · · · · · G3-10). 10% distorted grid in any direction may allow about 1.5% error on an average. But as shown in previous discussions, the error increases rapidly with increase of the distortion rate, so the error may remains less than 1% only for the 10% distorted grid.

As shown in the Fig. 4, the grid distortion in the high velocity field gives a significant effect on the gas flow. Thus in the high gas velocity region, the distortion of grids in other directions than that of the gas flow direction should be avoided or at least be reduced wherever possible.

4. Test and Discussion of Convection Schemes for Spray Calculations

Two convection schemes of Hybrid and Quick are applied and compared with each other. 20×20 square grids are chosen as the base grid to remove the effect of grid shapes, then four other grids based on the square grid are defined with 10°, 20°, 30° and 40° angles, as shown in Fig. 7(a).

For all the grids with different angles, the spray is injected in the direction normal to the wall in the same test conditions; injection pressure 5MPa, gas pressure 1.5MPa and gas temperature 288K.

The spray distributions are given in Fig. 7(b) and (c) and the velocity in Fig. 8. From the figures, the shapes of the spray by Quick or Hybrid are not apparently different from each other. But by looking carefully, for the square grid, the shape of spray returned by the Quick scheme is diffused rather more than by the Hybrid scheme. The gas field also shows the increased diffusive velocity by Quick. The reason is shown in Fig. 9. There is a high velocity gradient at the tip of sprays, thus the velocity on the east face by Quick scheme is not expressed correctly, i. e. negative ($u_e < 0$), different from the physical field. This negative flow on east face has a significant effect upon the u-velocity and v-velocity in the cell in that u_{ij} is reduced and v_{ij}, v_{ij+1} are increased.

In case of angled grids, the spray shapes by Quick have not shown any differences, but the shapes by Hybrid have shown that the front end of the sprays has been deflected to the side of the grids. That is also shown in the gas velocity distribution, i. e. the gas fields by Quick have gone straight down, not following the direction of the grid. However the gas fields by Hybrid are following the angled grid slightly, and have a lot

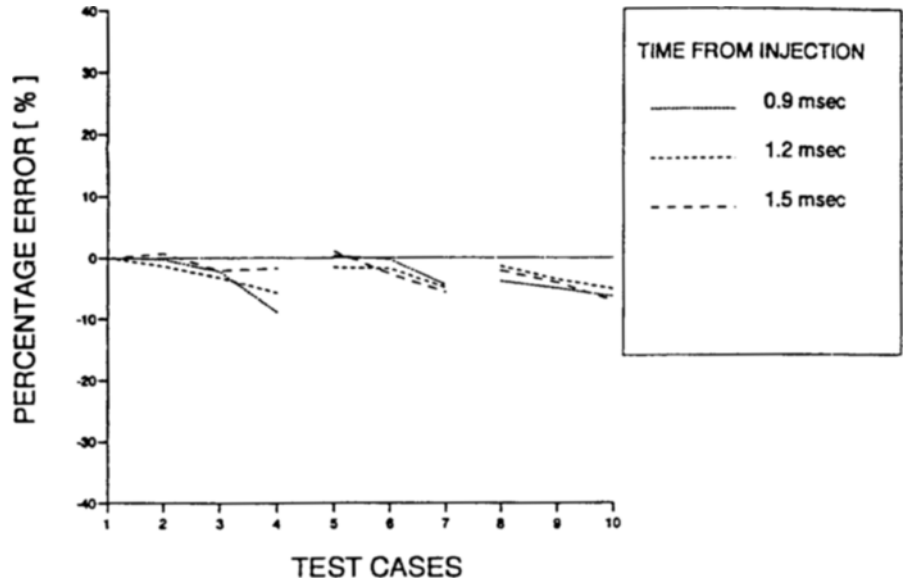

Fig. 6 Wall spray radius and height for case G1

of numerical diffusion associated with inclined grids.

The penetration curves of the sprays at 0.4ms from injection for the angled grids show in Fig.

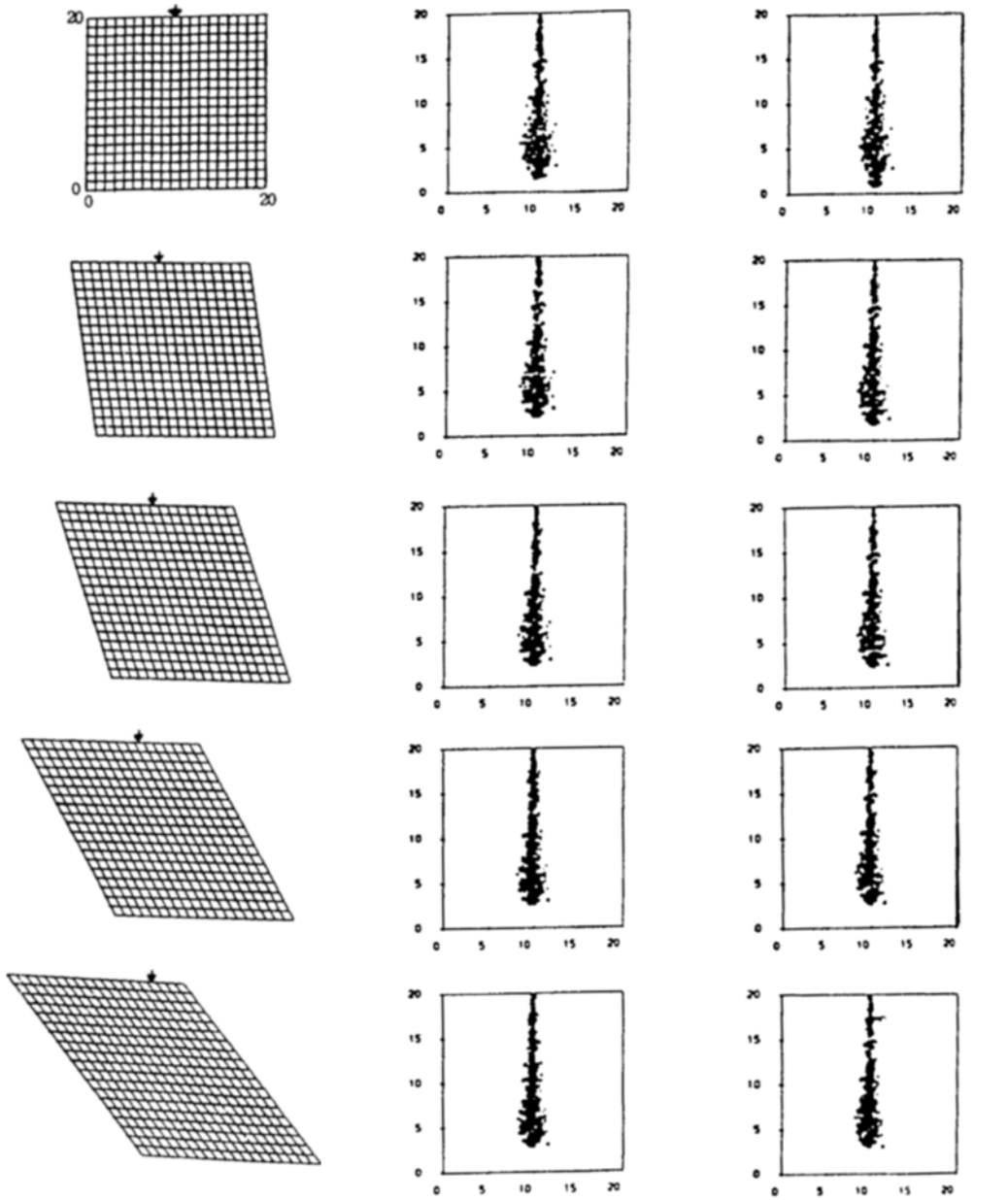

(a) Numerical grids (b) Droplet distributions(Quick) (c) Droplet distributions(Hybrid)

Fig. 7 Grid and droplet distrivutions

10 that Hybrid is better than Quick except for the large angled grid ($>30°$).

For the calculation of the spray injections, which always have large gradient regions at the front end, the Hybrid scheme with adaptive grids following the direction of spray/gas flow should

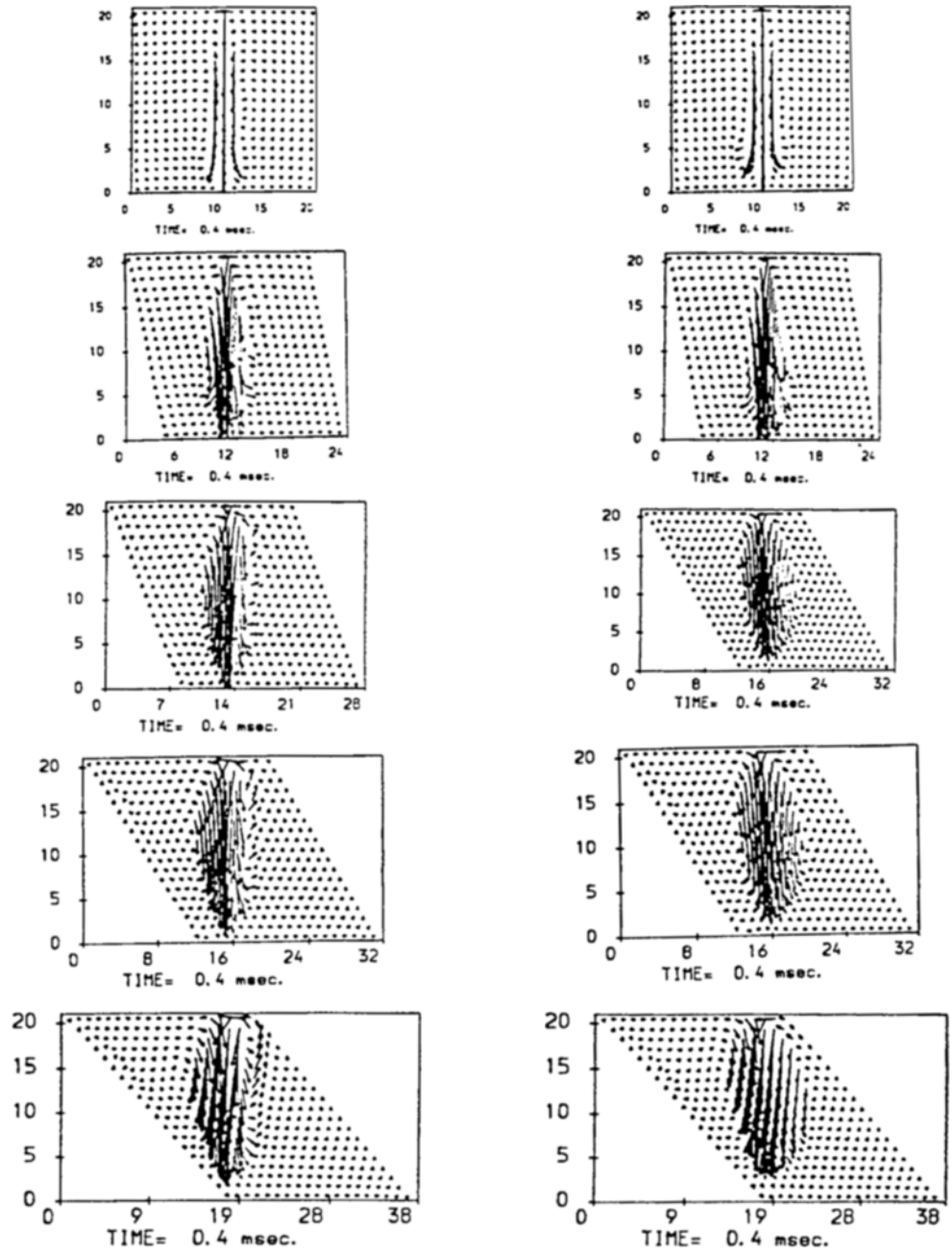

(a) Velocity distributions(Quick)

(b) Velocity distributions(Hybrid)

Fig. 8 Gas velocity distributions

be required.

5. Application on Shaped Chamber

New combustion chamber systems have been proposed by Kroeger(1986) and Kato and Onishi (1987) and also tested by Naber et al(1988). The basic geometry exhibit a raised surface at the centre of the piston bowl, onto which all of the fuel spray impacted.

In this section the grid effects are tested in the shaped diesel combustion chamber with a raised surface. High pressure injection is directed onto the land very close to the injector. Test conditions are given in Table 3. Shown in Fig. 11(a) (b) are the two different grids used, one follows the boundary surface and the other adaptive grid does not follow the boundary line but follows the spray/gas flow.

Figure 12(a) and(b) show the spray shape at 0.8ms after injection predicted by boundary following grid and by spray/gas flow adaptive grid respectively. The black thick curve gives the boundary occupied by the spray from the experimental results of Naber et al.(1988). In the case of the boundary following grid, the gas flow does not spread out into the free space but turns back into the centre, which is quite different from that in the experiment. On the contrary, the spray/gas flow following grid makes the spray distribution much like the experimental results.

Figure 13(a) and(b) show the gas flow fields at 0.8ms after injection predicted by boundary following grid and by spray/gas flow adaptive grid respectively. The gas flow shapes agree with the droplet distributions in Fig. 12. In the adaptive grid the gas flow spreads out on the level of the land, but that in boundary following grid returns into the main jet core with high velocities just after the edge of the land.

The chamber shape used in this section is only one example, sprays may occur in much more complex geometries. From the discussion it is clear that the grid following the boundary may give much worse predictions in the geometry with

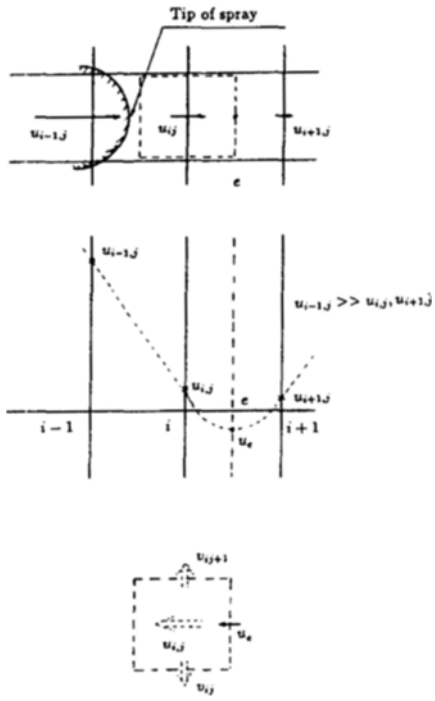

Fig. 9 Reason of more diffusion (Quick)

Table 3 Test condition

	Condition
Wall distance(mm)	6.43
Trap pressure(MPa)	3.2
Trap temperature(K)	760
Injection pressure(MPa)	91
Nozzle diameter(mm)	0.406
Bowl diameter(mm)	67.3
Max. depth(mm)	21.6

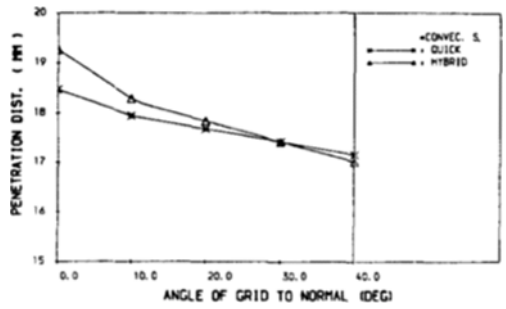

Fig. 10 Penetration vs. grid angle

shape edge which always has a big pressure gradient. Therefore, in those complex cases grids should follow the spray/gas flow, not the boundaries.

6. Conclusions

The numerical calculations of spray impinging on a wall have been increased, and their calculation geometries have become complex. The geometry may give rise to numerical errors. The following conclusions are drawn from the results presented in this paper,

(1) The spray shapes do not show any significant differences for various grid distortions, in particular the sprays before impaction have very similar shapes.

(2) The high velocity flows induced in jet

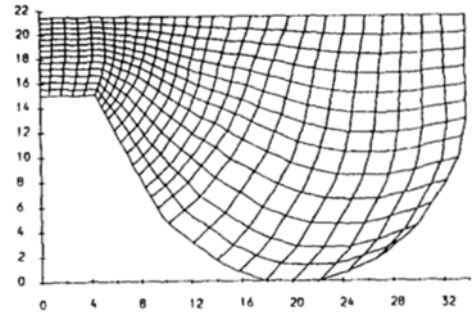

(a) Boundary following grid

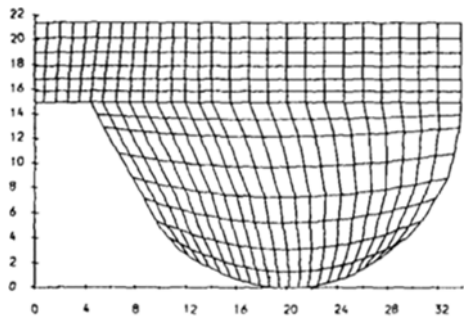

(b) Spray/gas flow following adaptive grid

Fig. 11 Grids to the shaped chamber tested

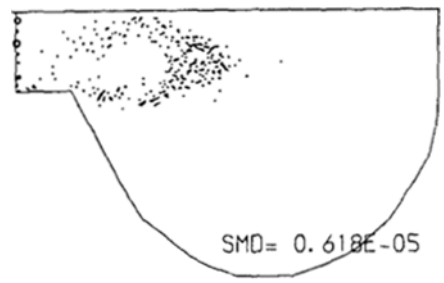

(a) In Boundary following grid

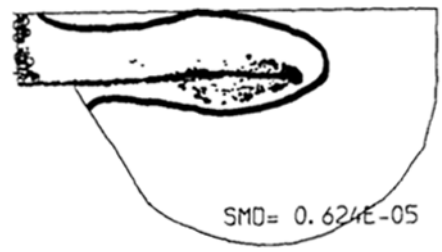

(b) In Spray/gas flow following adaptive grid

* Thick black line : Experimental results by Naber et al. (1988)

Fig. 12 Droplet distributions at 0.8ms from injection

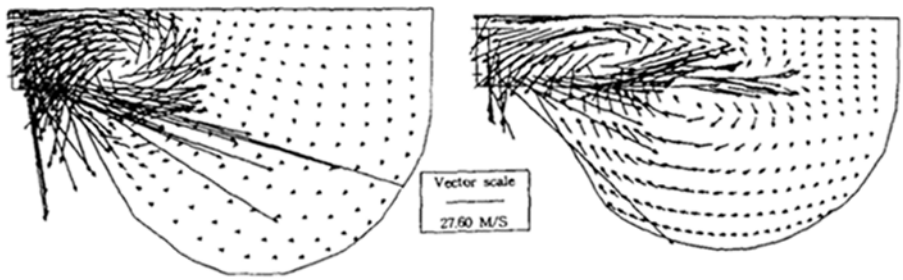

(a) In Boundary following grid

(b) In Spray/gas flow following adaptive grid

Fig. 13 Gas flow fields at 0.8ms from injection

region near the injector or wall jet region near the impingement wall make the gas flow irregular. The gas velocity fields are less orderly with distorted grids, but the overall gas flows are still similar.

(3) The free spray penetrations are affected by the pattern of grid distortion. For the horizontally distorted grids, the penetration decreases in proportion to the distortion rate, on the contrary that in vertically distorted grids increases.

(4) For the horizontally distorted grid cases the values of SMD after wall impaction increase in proportion to its distortion rate but the SMD decreases for the vertically distorted grids.

(5) Considering the differences in wall spray radius + height as the gross loss caused by the grid distortion, it increases with distortion rate. 10% distorted grid in any direction may cause about 1.5% error on average.

(6) The shapes of the spray returned by the Quick or Hybrid schemes are not apparently different from each other.

(7) For the square grid the shape of the spray/gas flow by the Quick scheme is diffused rather more than by the Hybrid scheme. In the case of angled grids, the spray shapes by Quick have not shown any differences, but the shapes by Hybrid have shown that the front end of the sprays has deflected to the side of the grids.

(8) With regards to the penetration of the sprays, Hybrid is better than Quick except for the large angled grid ($>30°$).

(9) For the calculation of the spray injections into chambers with complex boundaries, adaptive grids following the direction of spray/gas flow are required.

References

Crowe, C. T., Sharma, H. D. and Stock, D. E., 1977, "The Particle -Source- in Cell (PSI-cell) Model for Gas Droplet Flows," *ASME J. Fluid Engineering*, Vol. 99, pp. 325~332.

Dukowicz, J. K., 1980, "A Particle-Fluid Numerical Model For Liquid Sprays," *J. Comp. Phys.*, 35:229~233.

Fujimoto, H., Saito, M., Minoura, A., Katsura, W., Cho, I. and Senda, J., 1988, "Characteristics of a Diesel Spray Impinging on a Flat Wall," *Int. Conf. on Liquid Atomization and Spray Systems.*

Gosman, A. D., Ioannides, E., Lever, D. A. and Cliffe, K. A., 1980, "A Comparison of Continuum and Discrete Droplet Finite-Difference Models Used in the Calculation of Spray Combustion in Swirling Turbulent Flows," *AERE Harwell Report TD*865.

Kato, S. and Onishi, S., 1987, "New Mixture Formation Technology of Direct Fuel Injection Stratified Combustion SI Engine (OSKA)," *SAE Paper* 871689.

Kato, S. and Onishi, S., 1990, "New Type of Diesel Engine by impingement of Fuel Jet (OSKA -D)," *SAE Paper* 901618.

Khaleghi, H., 1990, "Three-Dimensional Modelling of Sprays and Gas Flow in Test Rigs and Diesel Engines and Comparison with Experiment," Ph.D. thesis, University of Manchester, Faculty of Technology.

Kroeger, C. A., 1986, "A Neat Methanol Direct Injection Combustion System for Heavy Duty Applications," *SAE Paper* 861169.

Naber, J., Enright, B. and Farrell, P., 1988, "Fuel Impingement in a Direct Injection Diesel Engine," *SAE Paper* 881316.

Ogura, M. and Lin, B., 1994, "A New Multi -Impingement-Wall Head Diffusion Combustion System (NICS-MH) of a d. i. Diesel Engine," *SAE paper* 940196.

Park, K., Wang, D. M. and Watkins, A. P., 1993, "A Contribution to the Design of a Novel Direct-Injection Diesel Engine Combustion System - Analysis of Pip Size," *Appl. Math. Modelling*, 17:114~124.

Park, K., 1996, "Assessment and Application of a New Spray Wall Impaction Model," *Computers in Reciprocating Engines and Gas Turbines, I. Mech. E*, pp. 1~10.

Watkins, A. P., 1989, "Three-Dimensional Modelling of Gas Flow and Sprays in diesel engines," In Markatos, N. C., editor, *Computer Simulation of Fluid Flow, Heat and Mass Transfer and Combustion in Reciprocating Engines*, pp. 193~237, Hemisphere.